Performance Gains of Single-Frequency Dual-Cell HSDPA

Danlu Zhang, Pavan Kumar Vitthaladevuni, Jilei Hou and Bibhu Mohanty, *Members IEEE*[1][2]

***Abstract*— In this paper, we will study the scheme of Single-Frequency Dual-Cell HSDPA (SF-DC HSDPA) which is introduced to simultaneously transmit two separate packet streams from two cells to a mobile. The inter-stream interference is suppressed by the linear-MMSE equalizer at the mobile. In the simple implementation studied in this paper, the schedulers at the two cells are independent without information exchange. Our study is based on both analysis and simulations. SF-DC HSDPA offers significantly higher data rates to users in the handover region. It also achieves dynamic load balancing in terms of resource utilizations across cells. Furthermore, all these gains can be obtained without degrading the performance of users not in handover and the legacy users. The gain from SF-DC is particularly substantial for users in heavily loaded cells surrounded by lightly loaded neighboring cells. In addition, such gain can increase with loading at a given loading ratio between the heavily loaded and lightly loaded cells. SF-DC is easy to implement with only incremental complexity to the current mobile and network equipment.**

***Index Terms*—WCDMA, HSPA+, Multi-Point Transmission, MIMO, Multi-cell MIMO, Load Balancing, LMMSE, bursty traffic**

I. INTRODUCTION

WCDMA is the most popular choice for 3G cellular systems. After its initial release in 1999, WCDMA has been subsequently enhanced [1]. Examples include the High Speed Downlink Packet Access (HSDPA) and Enhanced Uplink (EUL or HSUPA) [2] for fast packet switch data services in the downlink and uplink respectively. Recently, HSDPA/HSUPA has been further strengthened [2] by the backward compatible HSPA+, including 64QAM, MIMO, Dual Cell/Carrier-HSDPA (DC-HSDPA) and Multi-Carrier HSDPA. Further evolution of HSPA continues in parallel with the new OFDMA-based Long Term Evolution, or LTE. Each enhancement offers substantial improvements in data rates, user experience, and capacity.

MIMO can provide mobiles much higher data rates from the two-stream transmissions. However, two-stream transmissions require two degrees of freedom in space, which demands rich scattering and appropriate antenna separations. In the cellular system with tight antenna space at both the mobile and base station, antenna separations may be limited. In [3], a scheme of coordinated beam-forming from multiple cells is proposed, which offers phenomenal gains. But the coordinated beam-forming scheme requires joint processing across cells at the physical layer. In HSDPA, this requires inter-cell coordination every 2ms Transmission-Time-Interval (TTI). This may not be practical. It is high desirable to design a scheme with low incremental complexity to the existing equipments.

In this paper, we will introduce a multi-cell MIMO scheme where two cells transmit separate data packets to a UE in soft or softer handover [6]. In this scheme, there is only one transmit antenna needed in each cell. The scheme can be viewed as Per-Antenna-Rate-Control (PARC) across two cells. The packet scheduling at the two cells can be independent and thus joint processing at the physical layer is completely avoided. This scheme is called Single-Frequency Dual-Cell HSDPA (SF-DC), which is an important scheme of the Multi-Point HSDPA feature currently being studied by the 3GPP standards organization.

SF-DC can also be viewed as an extension of DC-HSDPA to the single-carrier network. SF-DC replaces the two carriers in DC-HSDPA by two cells in the same carrier.

This paper is organized as follows: in Section II, the SF-DC scheme is described and its benefits are discussed; in Section III, analytical results are presented for the SF-DC gain in a basic scenario; in Section IV, simulation results are provided to show the substantial benefit of SF-DC under practical network conditions; in Section V, concluding remarks are presented.

In this paper, we assume the readers have basic knowledge of WCDMA and HSPA, for which [1] is a good primer.

The terms ‘user’ and ‘UE’ are used interchangeably in this paper.

II. SF-DC CONCEPT AND BENEFITS

In a system with SF-DC, if a UE is in softer or soft handover, it will be served by both the primary serving cell (which has the strongest pilot Ec/Io), and the secondary serving cell (which has the second strongest pilot Ec/Io). In the baseline, all the UEs are served only by its primary serving cell. Typically, up to 50% of UEs in the WCDMA system are in handover. The difference between SF-DC and the conventional handover is that in the latter, the same data are transmitted by multiple cells whereas in SF-DC, the two packet streams from the two cells are independent. The inter-stream interference in SF-DC is suppressed by the UE with a Linear-MMSE equalizer [4].

[1] All the authors are with Qualcomm Inc., 5775 Morehouse Drive, San Diego, CA 92121. All correspondence should be addressed to Danlu Zhang (Phone: 858-6582703, fax: 858-8451254, e-mail: dzhang@qualcomm.com).

The SF-DC UE measures the channel quality of both cells and feeds back a Channel Quality Indicator (CQI) to them. Each serving cell schedules the packets independently without information exchange or joint processing at the physical layer. This 'per-cell rate control' is a multi-cell extension to the 'per-antenna rate control' (PARC) studied as a proposal for the single-cell MIMO for HSDPA Rel. 7[10].

In any TTI, one or two packets can be transmitted to the UE. The ACK/NAK for these packets are fed back to the cells for Hybrid ARQ operation. These are similar to DC-HSDPA by replacing the two carriers by two cells in the same carrier.

Thus, SF-DC can be seen as the fusion of multi-cell PARC-based MIMO and DC-HSDPA in a single carrier. SF-DC is closer to MIMO on the physical layer since the UE needs receive diversity and a LMMSE equalizer and the closed-loop data rate control mechanism is in the form of PARC. SF-DC is closer to DC-HSDPA on the MAC layer since it combines resources from multiple transmitting entities and the control channel messages, including CQI, ACK/NAK and HS-SCCH are encoded in the same format as in DC-HSDPA. In addition, the UE implementation for SF-DC is more likely to be based on DC-HSDPA capable UEs.

Figure 1 illustrates the basic operations in SF-DC.

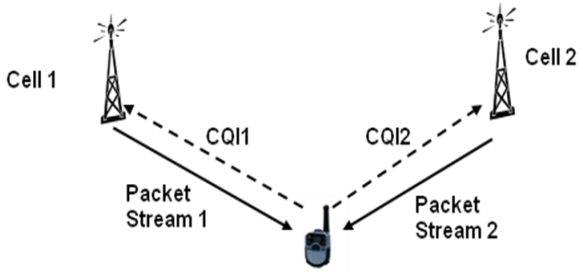

Figure 1: Basic operations in SF-DC

The benefit of SF-DC includes higher data rates for the users in the handover region and dynamic load balancing across the cells. The users in handover region achieve higher throughput from being served by two cells of similar channel quality. The load balancing gain with SF-DC first comes from the bursty nature of most data applications where the resource utilization of the cells changes dynamically and independently [11]. Furthermore, the loading across cells is often different. For example, two neighboring cells, one covering a business/industrial area and the other covering a residential area, may experience opposite periods of heavy and light loading. With SF-DC, the resource of available time slots from multiple cells is combined to provide gains of statistical multiplexing. As seen later, SF-DC gain is particularly substantial under non-uniform loading.

For the implementation, the mobiles capable for DC-HSDPA can decode data packets from two carriers. The same decoding capability can be applied to data packets from two cells in the same carrier. In addition, the CQI in DC-HSDPA reports channel quality of both carriers. The same CQI format can be used to report the channel quality of two serving cells in the same carrier. A UE with receive diversity and a Linear-MMSE equalizer can successfully suppress the inter-stream interference.

On the network side, SF-DC is a smooth migration. The schedulers at the two cells are independent. Furthermore, no transmit beam-forming from each cell is necessary. Since the cost of a second power amplifier is avoided, the deployment of SF-DC may be considered less expensive than that of single-cell MIMO based on transmit beam-forming.

One common issue with multiple packet streams is that the packets received by the mobile could be out-of-order. The impact can be eliminated by enhancements to the upper layer protocols. In the case of SF-DC, minor modifications are needed for the Radio Link Control protocol which handles link layer error recovery. These modifications were discussed in [6] and [12] and will not be studied here. The solutions to other practical issues like the decoding of the CQI feedback by the secondary serving cell are also addressed by [6]. Generally speaking, compared to the legacy system with a single serving cell and a single carrier, the power for the CQI feedback in SF-DC must be boosted to the same level as in DC-HSDPA where the UE receives services from a single cell but two carriers.

III. Basic Analysis

In this section, we analyze a basic single-user system. Assuming this single user is in handover between Cell 1 and 2.

Let's denote, at chip-level sampling time *n*, the transmitted pilot sample from Cell *i*, *i=1,2* as $p_i(n)$, pilot channel transmission power as $P_{p,i}$, transmitted data sample as $x_i(n)$, data channel transmission power as $P_{x,i}$. Let's denote the received samples by the UE at the two receive antennas as $y_j(n)$, *j=1,2*, in which the sum of total interference from cells other than Cell 1 and Cell 2, and thermal noise as $z_j(n)$, whose co-variance matrix is $\sigma_z^2 I_{2x2}$, where I_{2x2} is the identity matrix. Here $z_j(n)$ is assumed to be independent across the two receive antennas. In the following, we will call $z_j(n)$ simply as the 'noise' term.

After dispreading, the pilot and data become orthogonal, namely $\sum_{n=1}^{SF} x_i(n)\, p_i(n) = 0$, where *SF* is the spreading factor. The time index *n* is suppressed in the following to ease the presentation. Denoting the 1x2 channel for each cell as H_i, we have

$$y = \begin{pmatrix} y_1 \\ y_2 \end{pmatrix} = H_1(\sqrt{P_{p,1}}\, p_1 + \sqrt{P_{x,1}}\, x_1) + H_2(\sqrt{P_{p,2}}\, p_2 + \sqrt{P_{x,2}}\, x_2) + \begin{pmatrix} z_1 \\ z_2 \end{pmatrix}.$$

After de-spreading, the chip-level Signal-to-Interference-and-Noise-Ratio, achieved by the LMMSE equalizer, for the data channel from Cell *i*, denoted as SINR_i, is

$$\mathrm{SINR}_i = \frac{\Sigma_{x_i y} \Sigma_{yy}^{-1} \Sigma_{y x_i}}{1 - \Sigma_{x_i y} \Sigma_{yy}^{-1} \Sigma_{y x_i}} \tag{1}$$

where $\Sigma_{x_i y} = E(x_i\, y^H) = H_i^H P_{x,i}$ and

$$\Sigma_{yy} = E(yy^H) = [H_1 H_1^H (P_{p,1} + P_{x,1}) + H_2 H_2^H (P_{p,2} + P_{x,2}) + \sigma_z^2 I_{2x2}].$$

The above analysis is different from that of single-cell MIMO in HSDPA. In SF-DC, the two cells use different PN sequences and thus the inter-stream interference at the symbol level is reduced by the spreading factor. In MIMO in HSDPA, the two streams use the same PN sequence and channelization

code, and the de-spreading does not reduce the inter-stream interference [9].

If the single user is a legacy user served by Cell 1, both pilot and data are transmitted in Cell 1 and only the pilot is transmitted in Cell 2. The pilot is needed in all the cells to support mobility of all UEs. Denote the total cell transmit power as P_t, pilot transmit power as αP_t ($\alpha<1$) and data transmit power as $(1-\alpha)P_t$. If the Shannon code is used, the legacy user gets a throughput of

$$R_{legacy} = \log_2(1+\mathrm{SINR}_{1,\mathrm{legacy}}) \quad , \qquad (2)$$

where $\mathrm{SINR}_{1,\mathrm{legacy}}$ is computed from Eqn. (1) with $P_{p,1} = P_{p,2} = \alpha P_t$, $P_{x,1} = (1-\alpha)P_t$ and $P_{x,2} = 0$.

In SF-DC, both cells serve the same user, so we have

$$R_{SF-DC} = \log_2(1+\mathrm{SINR}_{1,\mathrm{SF\text{-}DC}}) + \log_2(1+\mathrm{SINR}_{2,\mathrm{SF\text{-}DC}}) \qquad (3)$$

where $\mathrm{SINR}_{\mathrm{i,SF\text{-}DC}}$ is computed from Eqn. (1) with $P_{p,1} = P_{p,2} = \alpha P_t$ and $P_{x,1} = P_{x,2} = (1-\alpha)P_t$.

From Eqn. (2) and (3), there is a degree of freedom gain in SF-DC but Cell 1 experiences increased interference from Cell 2 due to $P_{x,2}$. The impact from the increased interference is mitigated by LMMSE.

To compare the throughput for the legacy and SF-DC more quantitatively, we study a basic example where the channel is line of sight. Without losing generality, let $H_i = A_i \exp(j\phi_i)[1, \exp(j\theta_i)]^T$, with A_i as amplitude and θ_i and φ_i as phase offsets. Define the signal-to-'noise' ratio as $\gamma_i = A_i^2 P_t / \sigma_z^2$, we have

$$R_{legacy} = \log_2\left\{1+2(1-\alpha)\gamma_1 \frac{1+2\alpha\gamma_2 \sin^2[(\theta_1-\theta_2)/2]}{1+2\alpha\gamma_2}\right\};$$

$$R_{SF-DC} = \log_2\left\{1+2(1-\alpha)\gamma_1 \frac{1+2\gamma_2 \sin^2[(\theta_1-\theta_2)/2]}{1+2\gamma_2}\right\}$$

$$+\log_2\left\{1+2(1-\alpha)\gamma_2 \frac{1+2\gamma_1 \sin^2[(\theta_1-\theta_2)/2]}{1+2\gamma_1}\right\}.$$

Assuming θ_1 and θ_2 are uniformly distributed, we have the average gain of SF-DC at given (γ_1,γ_2) plotted in Figure 2 with α=0.3. When $\gamma_2>\gamma_1$, the legacy user will be served by Cell 2 and its throughput is computed by $\mathrm{SINR}_{2,\mathrm{legacy}}$ accordingly. Therefore, the gain is symmetric when γ_1 and γ_2 are swapped.

As seen in Figure 2, SF-DC always provides a throughput gain at any given (γ_1,γ_2). The gain is decreasing with $|\gamma_1-\gamma_2|$. In addition, the gain is increasing when the fraction of noise in the total interference decreases. For example, when $\gamma_1=\gamma_2$, the gain increases with γ_1.

In summary, Figure 2 shows that in SF-DC, with the help from the LMMSE spatial interference suppression, the increase in the degrees of freedom provides a net gain in the UE throughput despite the increased interference.

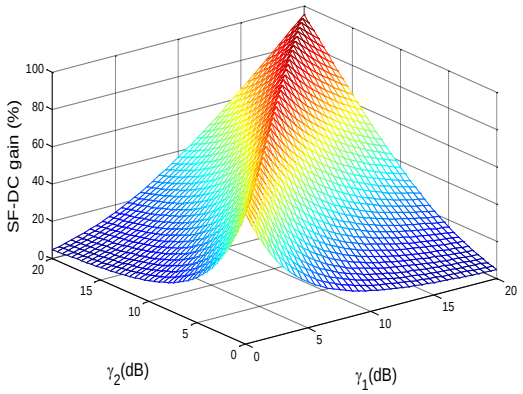

Figure 2: SF-DC gain in the basic two-cell scenario.

IV. Simulation Studies

This section is organized as follows: in subsection IV.A, we list the assumptions used in our simulations; in Section IV.B, we present the performance result when all the UEs are capable of SF-DC and the loading in the system is uniform; in Section IV.C, we present the performance result when all the UEs are capable of SF-DC and the loading in the system is non-uniform; in Section IV.D, we discuss the SF-DC gain as a function of loading and explain the trends observed in Section IV.B and IV.C; in Section IV.E, we present the performance result with a mix of legacy and SF-DC UEs under non-uniform loading.

A. Simulation assumptions

Table 1 lists the assumptions used in our study. These assumptions follow the methodology used by 3GPP in numerous standardization studies [7] for WCDMA/HSPA. In general, this is a multi-user multi-cell system where all the users are engaged in bursty traffic file downloading.

Table 1: Simulation Assumptions for SF-DC

Parameters	**Comments**
Cell Layout	Hexagonal grid, 19 Node B, 3 cells per Node B with wrap-around
Inter-site distance	1000 m
Carrier Frequency	2000 MHz
Path Loss	L=128.1 + 37.6log10(R), R in kilometers
Log Normal Fading	Standard Deviation : 8dB Inter-Node B Correlation:0.5 Intra-Node B Correlation :1.0
Max BS Antenna Gain	14 dBi
Antenna pattern	$A(\theta) = -\min\left[12\left(\frac{\theta}{\theta_{3dB}}\right)^2, A_m\right]$ θ_{3dB}= 70° A_m = 20 dB
Channel Model	Pedestrian A at 3km/h
CPICH Ec/Ior	-10 dB
Total Overhead power including pilot	30%
UE Antenna Gain	0 dBi
UE noise figure	9 dB
UE Receiver Type	Dual antenna w/ LMMSE; channel estimation realistically modeled

Parameters	Comments
CQI feedback delay	3 TTIs (6ms)
Maximum Cell Transmit Power	43 dBm
Traffic	Bursty Traffic with multiple file arrivals: File Size: fixed at 1Mbits Inter-arrival time: Exponential, Mean=5 seconds

In the simulations, the users are dropped into the entire system randomly. In each drop, the number of users in each cell is a random variable whose mean, averaged over multiple drops, is specified according to the given loading distribution, either uniform or non-uniform across the cells.

All the users are assumed as capable of SF-DC. The serving cells are determined by the UE's active set which contains all the cells which are within a range (say 6 dB) of average SINR to the strongest serving cell. If there is only one cell in a UE's active set, this UE is served by this single cell and thus is not in SF-DC. If there are multiple cells in a UE's active set, the strongest cell becomes the primary serving cell and the second strongest cell becomes the secondary serving cell. In our simulations, around 50% UEs are in SF-DC.

In our studies, the scheduler at the each cell is independent for the simplicity in implementation. With SF-DC, the users served by a cell can be classified into two classes: primary users are those who either are not in handover, i.e. have this cell as their sole serving cell, or have this cell as their primary serving cell, with another cell as the secondary serving cell; the secondary users are those who have this cell as their secondary serving cell. Within a cell, the traffic for the primary users is given absolute priority over the traffic for the secondary users, namely, a SF-DC user will not be scheduled in its secondary serving cell if there is any traffic for any primary users in that cell. This scheduling policy protects the legacy users and non-handover users from being adversely affected by SF-DC.

The above scheduling algorithm serves as a reference design. Other choices are possible. For example, the prioritization between the primary and secondary users can be configured differently to achieve different system fairness between the SF-DC and non-SF-DC users.

In our simulations, the scheduling priority for all the users in the same class (primary and secondary) is based on the Proportional Fair metric [4].

The main performance metric is the average burst rate [8]. For a burst(file), the burst rate is defined as s/t, where s is the burst size and t is the total burst delay, which is the time difference between the burst arriving at the cell and the completion of all the data transmission over the air interface. The total burst delay t includes both the transmission time and queue waiting time. The average burst rate can be computed as $E[s/t]$ for either a user or all the users.

It is worth noting that in our simulations, the CQI decoding at both serving cells is realistically modeled by cross-correlation based decoders.

B. Performance under uniform loading

Here the average number of users is same in all cells. As seen later, the performance gain from SF-DC is even higher under non-uniform loading.

There are two scenarios in our simulation: a legacy system and a system with SF-DC.

To provide insight on the SF-DC gain, Figure 3 shows the cumulative distribution function (CDF) of the average burst rate for all the users in the system when there is 1 user per cell. As seen in Figure 3, there is a significant gain due to SF-DC. Figure 4 shows the user burst rate gain as a function of geometry, defined as the ratio of the received power from the primary serving cell to the sum of total received power from all other cells and the thermal noise. High geometry means the UE is close to the cell center. Since the handover users are typically located near the cell edge, the gain from SF-DC is concentrated on users with low to medium geometries.

Compared to the legacy system, the system with SF-DC may increase the inter-interference experienced by the non-SF-DC UEs. However, the increased interference is mitigated by the LMMSE equalization across the two receive antennas. Furthermore, the SF-DC UEs stay in the system for shorter periods of time since their data are finished faster thanks to the throughput increase. Overall, there is no degradation of performance to any users including those who do not avail of this feature (users not in softer or soft handover). This is clearly seen in Figure 3 and Figure 4. Thus SF-DC improves the system fairness in addition to the user throughput.

It is worth noting that in [6], the fairness improvement is shown to be present even when the SF-DC UEs are mixed with legacy UEs with a single receive antenna and thus not capable to suppress the inter-cell interference.

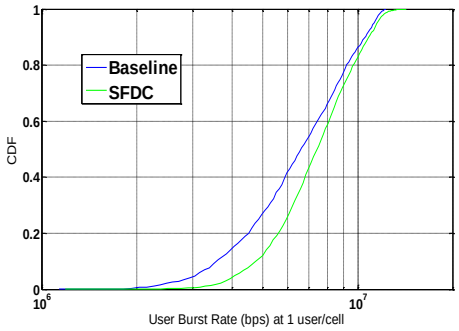

Figure 3: CDF of average user burst rates at 1 user/cell.

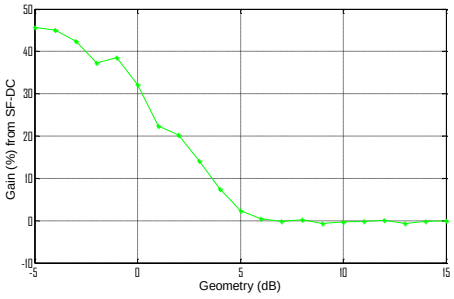

Figure 4: User burst rate gain vs. user geometry at 1 user/cell.

The performance with multiple users per cell is studied in Figure 5 and Figure 6. Figure 5 shows the average user burst

rate for handover users in the legacy and SF-DC systems. Figure 6 shows the burst rate gains for the handover users.

As an important aspect in a multi-user system, we will study the trend of SF-DC gain as a function of loading. In Figure 6, the gain from SF-DC decreases with loading. More analysis on this trend will be discussed later, especially after the results under non-uniform loading are presented.

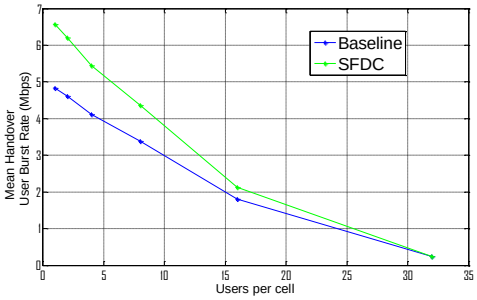

Figure 5: Average burst rate for handover UEs.

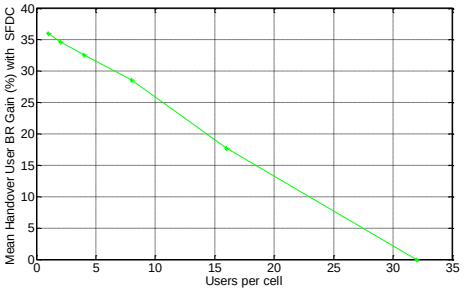

Figure 6. Gain in average burst rates for handover UEs.

C. *Performance under non-uniform loading*

In a real deployment, the system is often non-uniformly loaded as evidenced by data from the field. Consider the case where a UE's serving cell is heavily load over a given period of time, while a neighboring cell (in UE's active set) is more lightly loaded during the same period. With SF-DC, this UE would get scheduled from both the cells thereby resulting in dynamic load-balancing. Without SF-DC, such a UE would only get scheduled from the heavily loaded serving cell and thereby experiences poorer performance while the lightly loaded neighboring cells would not be efficiently utilized.

To analyze gains in this scenario, we have assumed, on average, 3 cells in the center of the 57-cell system have 3*N users/cell, while the other 54 cells have N users/cell. Figure 7 and Figure 8 below focus on the performance of UEs in the heavily loaded center cells. The SF-DC UEs in the lightly loaded cells experience smaller but positive gain.

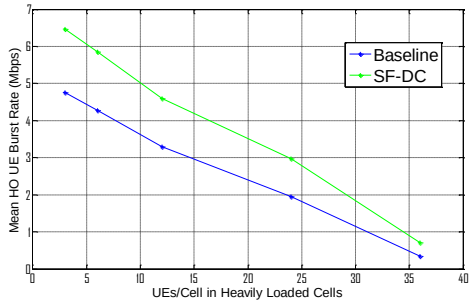

Figure 7: Average burst rate for handover UEs in the heavily loaded cells.

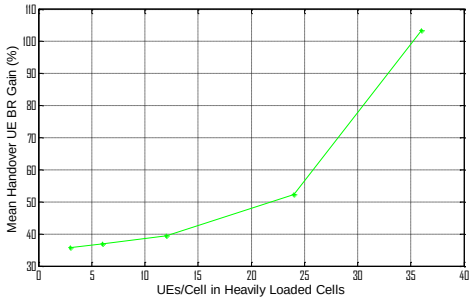

Figure 8: Average burst rate gain for handover UEs in the heavily loaded cells.

Figure 7 shows the average burst rate of handover UEs in the heavily loaded center cells with and without SF-DC. Figure 8 shows the average burst rate gain for these UEs with SF-DC. Here gain in excess of 100% is observed.

From Figure 7 and Figure 8, two important trends can be identified:

1. The gain from SF-DC is higher in the highly loaded cells in the non-uniformly loaded system than in a cell in a uniformly loaded system. This is seen by comparing the gains in Figure 8 and Figure 6 at the same number of users in the cell. This is because the handover UEs in the highly loaded cells can get more service from the lightly loaded neighboring cells.
2. The gain from SF-DC for UEs in the heavily loaded cells increases with load. This is different from Section IV.B with uniform loading. The reason is analyzed in the next subsection.

D. *SF-DC gain as a function of loading*

In our simulations with non-uniform loading, the loading ratio between the lightly loaded cells to the heavy loaded cells is kept constant. Qualitatively, the service from the secondary serving cell decreases much slower with increasing load since the neighboring cells are much less loaded. Thus, as load increases, a SF-DC UE in the heavily loaded cell receives an increasing portion of its total service from its lightly loaded secondary serving cell.

To be more quantitative, we will approximate the system by a M/M/1 queuing system [5]. The Inter-burst arrival time itself is exponentially distributed. Let's assume the service time for a legacy user also follows the exponential distribution. Denote the mean arrival rate as λ and mean service rate as μ. In this M/M/1 queuing system, the mean total download time for a legacy user is $T_{legacy}=1/(\mu-\lambda)$.

With SF-DC, a handover user is also served by a neighboring cell when that cell is 'idle', namely, free from traffic of primary users. The arrival rate of primary users' traffic to the neighboring cell is $\eta\lambda$, where η is the loading ratio between the neighboring cell to this cell. The probability of the neighboring cell being idle is $(1-\eta\lambda/\mu)$ due to our priority scheduling. Assume the average user service rate increases from μ to $\mu+\beta\mu(1-\eta\lambda/\mu)$ where the gain factor β depends on the channel quality, loading, etc. In the new M/M/1 system, we have

$$T_{SF\text{-}DC} = \frac{1}{\mu + \beta\mu(1-\eta\lambda/\mu) - \lambda} = \frac{T_{legacy}}{1+\beta\dfrac{1-\eta(\lambda/\mu)}{1-(\lambda/\mu)}} \quad (4)$$

With uniform loading, $\eta=1$, and $T_{SF\text{-}DC} = T_{legacy}/(1+\beta)$. Typically β decreases with loading, since higher load leads to higher interference from those non-serving cells, reducing the inter-stream interference suppression efficiency of the LMMSE equalizer. This is seen in Figure 2. Thus the gain from SF-DC decreases with loading when the loading is uniform across the cells as in Section IV.B.

With non-uniform loading, for those heavily loaded cells, $\eta<1$. Let $G = \dfrac{1-\eta(\lambda/\mu)}{1-(\lambda/\mu)}$. Here *G* decreases with loading. For example, in Section IV.C, $\eta=1/3$ for the heavily loaded center cells; when a center cell is 30% loaded, its non-center neighboring cell is only 10% loaded, $G=9/7$; when the center cell is 90% loaded, the neighboring cell is only 30% loaded, $G=7$. This leads to a larger percentage of gain or latency reduction from SF-DC when loading increases.

E. Performance with a mix of SF-DC capable and legacy UEs

In this subsection, we assume 30% of UEs are SF-DC capable and the rest 70% of UEs are legacy UEs. The system loading is non-uniform as in Section IV.C.

In this study, a legacy UE has a single antenna and its LMMSE equalizer can only equalize the channel in the temporal domain. The assumption of no receive diversity at the legacy UEs represents a upper bound of the SF-DC impact on the legacy UEs since the increased inter-cell interference from SF-DC cannot be suppressed by the legacy UE.

Figure 9 shows the burst rate for all the SF-DC capable users with 3 and 24 UEs/cell in heavily loaded cells. As shown in the figure, SFDC operation helps improve burst rates. The gains increase from 3 users/cell to 24 users/cell, as expected based on the discussion in Section IV.D.

Figure 10 below shows the CDF of burst rate for legacy UEs. As seen clearly in Figure 10, they do not experience performance loss from the SF-DC operations. Despite the increased inter-cell interference when a SF-DC UE is served by two cells, the data of this SF-DC UE is finished faster due to the throughput increase. Therefore, overall, the legacy UE does not lose performance even without receive diversity.

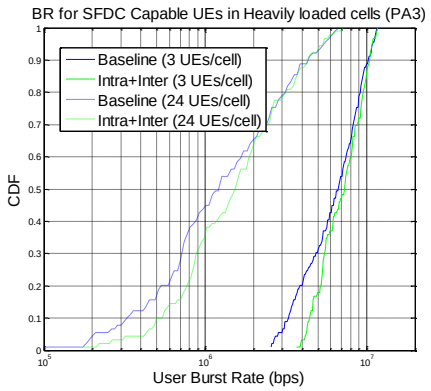

Figure 9: SFDC capable User Burst Rate CDF

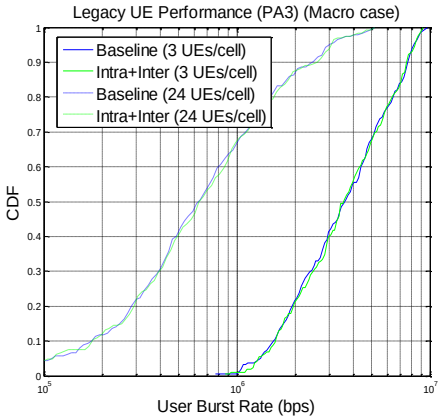

Figure 10: Burst Rate CDF for Legacy UEs in heavily loaded cells

V. CONCLUSION

SF-DC HSDPA has recently attracted considerable interest from the cellular industry. In this paper, we studied performance of SF-DC through both analysis and simulations. As seen in this paper, SF-DC provides promising gains in both user experience and system load balancing. System fairness is also improved since users who are not in handover region and thus cannot use SF-DC do not experience any performance degradation. In addition, the legacy UEs are not adversely affected by SF-DC. Moreover, the SF-DC gain is much more significant for UEs in the heavily loaded cells surrounded by lightly loaded cells. In our simulation, a user burst rate gain in excess of 100% is seen for UEs in the cells where the loading is three times that of some of its neighbors.

Our future work includes studying the SF-DC gain with UE mobility and extensions of the SF-DC scheme.

REFERENCES

[1] H. Holma and A. Toskala, "*WCDMA for UMTS: Radio Access for Third Generation Mobile Communications*", 3 ed, Wiley, 2004.

[2] E. Dahlman, S. Parkvall, J. Skold and P. Beming, "*3G Evolution: HSPA and LTE for Mobile Broadband*", 2nd ed., Academic Press, 2008.

[3] G.J. Foschini, K. Karakayali and R.A. Valenzuela, "Coordinating multiple antenna cellular networks to achieve enormous spectral efficiency", *IEE Proc. Commun.*, vol. 153, no. 4, Aug. 2006.

[4] D. Tse and P. Viswanath, "*Fundamentals of Wireless Communication*", Cambridge University Press, 2005.

[5] Dimitri P. Bertsekas and R. Gallager, *"Data Networks"*, 2ed.

[6] R1-104157, "On deploying DC-HSDPA UEs in Single Frequency Networks", 3GPP document by Qualcomm, RAN1#61-bis., 2010.

[7] R1-110563, "Simulation Framework for System Evaluation of Multi-Point HSDPA", 3GPP document, by Qualcomm, Ericsson, ST-Ericsson, Nokia Siemens Networks, Nokia, Huawei, HiSilicon, ZTE, 2011.

[8] Danlu Zhang, P. K. Vitthaladevuni, B Mohanty and Jilei Hou, "Performance analysis of Dual-Carrier HSDPA", in *VTC'10 Spring*.

[9] V. Chande, Haitong Sun, P. K. Vitthaladevuni, Jilei Hou and B. Mohanty, "Performance Analysis of 64-QAM and MIMO in Release 7 WCDMA (HSPA+) Systems", in *VTC'10 Spring*.

[10] 3GPP TR25.876, "Multiple Input Multiple Output (MIMO) antennae in UTRA"(study report), v 7.0.0, 2007.

[11] Manohar Naidu Ellanti, Steven Scott Gorshe, Lakshmi G. Raman, Wayne D. Grover, *"Next Generation Transport Networks: Data, Management, and Control Planes"*, Springer, 2005.

[12] "MultiPoint HSPA"(http://www.qualcomm.com/umts) , white paper, Qualcomm Inc., February, 2011.